

Efficient Implementation of LinearUCB through Algorithmic Improvements and Vector Computing Acceleration for Embedded Learning Systems

MARCO ANGIOLI, MARCELLO BARBIROTTA, ABDALLAH CHEIKH, ANTONIO MASTRANDREA, FRANCESCO MENICHELLI, and MAURO OLIVIERI, Department of Information Engineering, Electronics and Telecommunications (DIET), Sapienza University of Rome, Italy

As the Internet of Things expands, embedding Artificial Intelligence algorithms in resource-constrained devices has become increasingly important to enable real-time, autonomous decision-making without relying on centralized cloud servers. However, implementing and executing complex algorithms in embedded devices poses significant challenges due to limited computational power, memory, and energy resources. This paper presents algorithmic and hardware techniques to efficiently implement two LinearUCB Contextual Bandits algorithms on resource-constrained embedded devices. Algorithmic modifications based on the Sherman-Morrison-Woodbury formula streamline model complexity, while vector acceleration is harnessed to speed up matrix operations. We analyze the impact of each optimization individually and then combine them in a two-pronged strategy. The results show notable improvements in execution time and energy consumption, demonstrating the effectiveness of combining algorithmic and hardware optimizations to enhance learning models for edge computing environments with low-power and real-time requirements.

CCS Concepts: • **Computer systems organization** → **Embedded systems**; • **Computing methodologies** → **Machine learning**; **Online learning settings**; • **Theory of computation** → **Mathematical optimization**; • **Hardware** → **Hardware accelerators**.

Additional Key Words and Phrases: LinearUCB Algorithms, Sherman-Morrison-Woodbury Formula, Vector Hardware Acceleration, Embedded AI Optimization

ACM Reference Format:

Marco Angioli, Marcello Barbirotta, Abdallah Cheikh, Antonio Mastrandrea, Francesco Menichelli, and Mauro Olivieri. 2025. Efficient Implementation of LinearUCB through Algorithmic Improvements and Vector Computing Acceleration for Embedded Learning Systems. 1, 1 (January 2025), 22 pages.

1 Introduction

Artificial Intelligence (AI) is introducing innovative solutions and possibilities for problem-solving and automation across diverse domains, ranging from healthcare [32] to smart manufacturing [31], and autonomous driving [6]. In recent years, the rise of the Internet of Things (IoT) highlighted the necessity of embedding AI algorithms directly into small, everyday devices, transforming them into smart, autonomous units capable of reacting to the environment and making fast decisions without relying on centralized cloud servers [12, 29]. However, implementing and running complex AI algorithms on embedded systems poses significant challenges, particularly due to their limited computational power and energy [1].

Authors' Contact Information: [Marco Angioli](mailto:marco.angioli@uniroma1.it), marco.angioli@uniroma1.it; [Marcello Barbirotta](mailto:marcello.barbirotta@uniroma1.it), marcello.barbirotta@uniroma1.it; [Abdallah Cheikh](mailto:abdallah.cheikh@uniroma1.it), abdallah.cheikh@uniroma1.it; [Antonio Mastrandrea](mailto:antonio.mastrandrea@uniroma1.it), antonio.mastrandrea@uniroma1.it; [Francesco Menichelli](mailto:francesco.menichelli@uniroma1.it), francesco.menichelli@uniroma1.it; [Mauro Olivieri](mailto:mauro.olivieri@uniroma1.it), mauro.olivieri@uniroma1.it, Department of Information Engineering, Electronics and Telecommunications (DIET), Sapienza University of Rome, Rome, Italy, Italy.

© 2025

Manuscript submitted to ACM

Manuscript submitted to ACM

1

This paper addresses these challenges, introducing algorithmic and hardware optimization strategies, which can be applied independently or combined, to reduce complexity and enhance the execution time and energy efficiency of two LinearUCB Contextual Bandits algorithms: the Disjoint and the Hybrid [26].

On the algorithmic side, the resource-intensive process of updating and inverting the matrix underlying the learning process of these models is replaced by a more efficient, incremental update mechanism based on the Sherman-Morrison-Woodbury formula [33]. While this principle has been adopted in previous works to implement the Disjoint LinearUCB algorithm [17, 18, 36], in this paper, we extend this technique to a more complex Hybrid variant and thoroughly assess the impact of the incremental update on the complexity, execution time, memory requirements, and energy consumption of the LinearUCB algorithms across different embedded platforms.

On the other hand, looking at the hardware perspective, we leveraged the low-power Klessydra-T13 RISC-V processor’s built-in vector hardware accelerator as a case study to demonstrate the impact of vector computing support on enhancing the speed of matrix operations, which are essential for optimizing algorithm performance.

Combining these two approaches significantly boosts the execution speed of the algorithms while reducing their complexity, memory requirements and energy consumption, representing a major advancement in their applicability in resource-constrained settings with low-power and real-time requirements.

The rest of the work is organized as follows. Section 2 presents the LinearUCB algorithms and their applications in edge computing environments. Section 3 details the proposed algorithmic optimizations and discusses the achieved computational complexity reduction. Section 4 introduces the target RISC-V processor, focusing on the vector computing accelerator and its custom instruction set extension, which is exploited to further speed up the algorithms. Section 5 presents the results, discussing speedup and reduction in dynamic energy consumption. Finally, Section 6 summarizes the main outcomes of the work.

2 Background and Related Works

2.1 Background

Contextual multi-armed Bandits (CB) are a class of algorithms employed in sequential decision-making problems, in which the system must select the optimal action based on a given context [11, 26]. These algorithms operate on line, using a learning procedure based on a rewarding mechanism. At each time step, the algorithm observes the context, picks an action and receives a reward related to the chosen option. The reward is then used to update the model parameters so that the algorithm can adapt and learn at run time, gathering enough information to predict the relationship between the observed context and the reward associated with each action. Differently from Reinforcement learning (RL) scenarios, where actions influence subsequent states, and the objective is to maximize cumulative rewards over multiple state transitions, in CB problems, the selected action does not affect the next state, and the algorithm aims to maximize the immediate rewards at each iteration [5, 11, 13, 27].

One branch of CB algorithms is the LinearUCB presented in [26], subdivided into the Disjoint and Hybrid versions, each with different applications and advantages. The algorithms use the Upper Confidence Bound (UCB) [7] exploration strategy and assume a linear relationship between the context and the reward. At each time step t , the algorithm observes a set \mathcal{A}_t of N possible actions (or arms) together with their context feature vectors $\mathbf{x}_{t,a}$ for $a \in \mathcal{A}_t$. For a given action a , the expected reward is estimated based on the context $\mathbf{x}_{t,a}$, utilizing a ridge regression procedure. In the following, bold symbols are used to denote vectors and matrices, while scalar values are represented using regular (non-bold) symbols for clarity.

The *Disjoint LinearUCB algorithm* represents the simplest form of this approach, where each of the N possible actions is treated as an independent entity. In this model, the action is analytically represented through a $d \times d$ matrix \mathbf{A}_a and a $d \times 1$ vector \mathbf{b}_a , where d denotes the size of the context feature vector $\mathbf{x}_{t,a}$, without shared elements among actions. At every step, the algorithm employs the ridge regression in (1) to estimate the expected reward for each action and select the one with the highest value.

$$\begin{aligned}\hat{\boldsymbol{\theta}}_a &= \mathbf{A}_a^{-1} \mathbf{b}_a \\ p_{t,a} &= \hat{\boldsymbol{\theta}}_a^\top \mathbf{x}_{t,a} + \alpha \sqrt{\mathbf{x}_{t,a}^\top \mathbf{A}_a^{-1} \mathbf{x}_{t,a}}\end{aligned}\quad (1)$$

Based on the chosen option, the environment yields a reward to the model, which is subsequently employed to update the matrices associated with the selected action, as outlined in (2).

$$\begin{aligned}\mathbf{A}_{a_t} &= \mathbf{A}_{a_t} + \mathbf{x}_{t,a_t} \mathbf{x}_{t,a_t}^\top \\ \mathbf{b}_{a_t} &= \mathbf{b}_{a_t} + r_t \mathbf{x}_{t,a_t}\end{aligned}\quad (2)$$

The *Hybrid LinearUCB algorithm* is more complex than its Disjoint counterpart because it represents each action using a feature vector of size f , which encapsulates information common across all actions. Additionally, it employs a shared $k \times k$ matrix \mathbf{A}_0 and a shared $k \times 1$ vector \mathbf{b}_0 , where k is the product of the context and action feature vector lengths, f and d . Each action in the Hybrid algorithm is modelled using a $d \times d$ matrix \mathbf{A}_a , a $d \times k$ matrix \mathbf{B}_a , and a $d \times 1$ vector \mathbf{b}_a . The ridge regression in this model, as outlined in (3), accounts for the interaction between context and action features through the $\mathbf{z}_{t,a}$ vector in \mathbb{R}^k .

$$\begin{aligned}\hat{\boldsymbol{\beta}} &= \mathbf{A}_0^{-1} \mathbf{b}_0 \\ p_{t,a} &= \mathbf{z}_{t,a}^\top \hat{\boldsymbol{\beta}} + \mathbf{x}_{t,a}^\top \hat{\boldsymbol{\theta}}_a + \alpha \sqrt{s_{t,a}}\end{aligned}\quad (3)$$

After selecting an action, the associated and shared matrices are updated with the received reward, as per (4), (5) and (6). Equations (4) and (6) handle the updating of shared matrices, while (5) is specifically dedicated to updating the matrices associated with the selected action.

$$\begin{aligned}\mathbf{A}_0 &= \mathbf{A}_0 + \mathbf{B}_{a_t}^\top \mathbf{A}_{a_t}^{-1} \mathbf{B}_{a_t} \\ \mathbf{b}_0 &= \mathbf{b}_0 + \mathbf{B}_{a_t}^\top \mathbf{A}_{a_t}^{-1} \mathbf{b}_{a_t}\end{aligned}\quad (4)$$

$$\begin{aligned}\mathbf{A}_{a_t} &= \mathbf{A}_{a_t} + \mathbf{x}_{t,a_t} \mathbf{x}_{t,a_t}^\top \\ \mathbf{B}_{a_t} &= \mathbf{B}_{a_t} + \mathbf{x}_{t,a_t} \mathbf{z}_{t,a_t}^\top \\ \mathbf{b}_{a_t} &= \mathbf{b}_{a_t} + r_t \mathbf{x}_{t,a_t}\end{aligned}\quad (5)$$

$$\begin{aligned}\mathbf{A}_0 &= \mathbf{A}_0 + \mathbf{z}_{t,a_t} \mathbf{z}_{t,a_t}^\top - \mathbf{B}_{a_t}^\top \mathbf{A}_{a_t}^{-1} \mathbf{B}_{a_t} \\ \mathbf{b}_0 &= \mathbf{b}_0 + r_t \mathbf{z}_{t,a_t} - \mathbf{B}_{a_t}^\top \mathbf{A}_{a_t}^{-1} \mathbf{b}_{a_t}\end{aligned}\quad (6)$$

The Hybrid algorithm imposes considerably higher memory requirements and computational demands, potentially presenting challenges for its direct deployment in resource-constrained embedded environments. However, including shared matrices in the Hybrid model enables the estimation of rewards for context-action tuples that have not been tested yet but are similar to those previously explored [26]. This enhancement substantially accelerates the convergence time for the algorithm, particularly in scenarios with strong correlations among actions.

Notably, unlike RL algorithms such as Q-learning [11, 13], which update state-action values with scalar adjustments, LinearUCB algorithms heavily rely on matrix operations at each step, motivating the optimizations introduced in this work.

2.2 Related Works

Contextual Bandits algorithms have demonstrated their versatility across a wide range of applications. In healthcare and biology, these algorithms have been applied to improve treatment allocation in clinical trials [20] and propose personalized dosing strategies [10]. In recommendation systems, they found notable applications in personalizing article selection or tailoring movie recommendations like for Yahoo homepages [26] and Netflix [2] respectively, demonstrating the ability to learn user preferences over time, enhancing the experience and engagement [11, 23, 26, 34]. Furthermore, recent advancements have shown the potential of LinearUCB algorithms in enhancing hardware efficiency. The study in [5] employs these algorithms to automatically select the optimal configuration of a general-purpose hardware accelerator according to the workload and reconfigure the architecture at run-time.

Recently, Contextual Bandit algorithms have also emerged in edge computing environments for localized data processing and real-time decision-making. The work in [34] proposes using CB algorithms directly executed on mobile phones or wearable devices for mobile health, personalizing interventions based on user context such as GPS location, calendar busyness, and heart rate. This approach ensures interventions can occur even in network issues or failures, providing robust and timely support. It also addresses privacy concerns by keeping sensitive health data localized on the user’s device. In [14], authors employ CB algorithms on resource-constrained nanodrones to dynamically allocate inference tasks between edge and cloud, based on predicted network delays. This approach demonstrates improved adaptability in task allocation, enabling efficient computation offloading and optimized edge computing in fluctuating network conditions. The work in [16] proposes a CB approach to optimize the placement of services on edge nodes, enhancing response times and service quality for users. Their algorithm runs directly on edge devices and dynamically rents computing resources based on spatial and temporal demand patterns, adapting to changes in user needs across different times and places. [35] proposes a CB algorithm to split tasks across multiple edge devices, selecting the most reliable ones in real-time. This ensures stable, deadline-driven performance even in fluctuating network conditions, making it ideal for large-scale, distributed edge applications. In the context of emerging networks, authors in [25] utilize CB to optimize intelligent and secure radio environments in 6G vehicular-aided heterogeneous networks, demonstrating their potential to enhance the efficiency and security of these advanced networks. In all these contexts. All these applications require CB algorithms to be implemented efficiently and meet the demands of resource-constrained systems, ensuring minimal impact on device performance and battery life [34].

While many efforts have been made in the literature to explore possible applications of CB algorithms and improve their accuracy, no previous study investigated approaches to reduce the computational complexity and the requirements of LinearUCB algorithms for implementation on edge devices with low-power and real-time requirements. This paper aims to fill this gap by exploring and developing software and hardware approaches that specifically reduce CB computational load and resource demands, making them more feasible and efficient for use in resource-constrained edge computing environments.

3 Algorithmic Optimizations

The LinearUCB algorithms rely on the linearity assumption between the context and the reward, employing ridge regression procedures to assess the expected reward for each action and determine the optimal one.

The key point of this process is matrix inversion, a computationally intensive operation whose complexity grows cubically with the size of the matrix. The Disjoint LinearUCB requires inverting N matrices of dimensions $d \times d$ at each step, for an asymptotic complexity equal to $O(d^3)$. The Hybrid variant is even more demanding, requiring the

Algorithm 1 Optimized Disjoint LinearUCB

```

1: Input:  $\alpha \in \mathbb{R}_+$ 
2: for  $t = 1, 2, \dots, T$ 
3:   Observe the context for all arms  $a \in \mathcal{A}_t$ :  $\mathbf{x}_{t,a} \in \mathbb{R}^d$ 
4:   for all  $a \in \mathcal{A}_t$ 
5:     if  $t=1$ :
6:        $\mathbf{A}_a^{-1} = \mathbf{I}_d$ 
7:        $\mathbf{b}_a = \mathbf{0}_{d \times 1}$ 
8:     endif
9:      $\hat{\boldsymbol{\theta}}_a = \mathbf{A}_a^{-1} \mathbf{b}_a$ 
10:     $p_{t,a} = \hat{\boldsymbol{\theta}}_a^\top \mathbf{x}_{t,a} + \alpha \sqrt{\mathbf{x}_{t,a}^\top \mathbf{A}_a^{-1} \mathbf{x}_{t,a}}$ 
11:  endfor
12:  Choose  $a_t = \arg \max_{a \in \mathcal{A}_t} (p_{t,a})$ 
13:  and observe a real-valued payoff  $r_t$ 
14:   $\mathbf{A}_{a_t}^{-1} = \mathbf{A}_{a_t}^{-1} - \frac{\mathbf{A}_{a_t}^{-1} \mathbf{x}_{t,a} \mathbf{x}_{t,a}^\top \mathbf{A}_{a_t}^{-1}}{1 + \mathbf{x}_{t,a}^\top \mathbf{A}_{a_t}^{-1} \mathbf{x}_{t,a}}$ 
15:   $\mathbf{b}_{a_t} = \mathbf{b}_{a_t} + r_t \mathbf{x}_{t,a_t}$ 
16: endfor

```

inversion of a large $k \times k$ and $N d \times d$ matrices, asymptotically growing as $O(k^3) = O(f^3 d^3)$. This operation, common to both algorithmic variants, imposes a heavy computational load, resulting in performance bottlenecks and significant challenges for real-time applications where rapid decision-making is crucial. To mitigate this problem, the approach in [26] proposes to update the original matrices at each step while computing and caching the inverses periodically instead of in real-time. However, this approach may limit online learning capabilities due to less frequent model updates, requires more memory and still necessitates longer iterations at regular intervals.

Given that matrix inversion constitutes a bottleneck affecting the scalability and efficiency of LinearUCB algorithms, this section describes and explores mathematical strategies that can yield the same results without relying on this operation. First, we discuss the modifications applied to the simpler Disjoint LinearUCB algorithm, where the same principle has been adopted in previous works [17, 18, 21, 28, 36], and then we extend the approach to the more complex Hybrid model. For each variant, we thoroughly investigate the impact of the proposed techniques on the computational complexity, execution time, energy consumption, and memory requirements, which are essential aspects for applications on embedded systems, while varying the problem parameters.

3.1 Optimization of the Disjoint LinearUCB through the Sherman-Morrison Formula

In the Disjoint algorithm, the \mathbf{A}_a matrices are utilized in their inverted form, \mathbf{A}_a^{-1} , during action selection and subsequently adjusted in the normal form during the update phase based on the received reward. However, the process of updating and then inverting the matrix in each iteration introduces computational inefficiencies, especially as the matrix size increases.

Considering that \mathbf{A}_a undergoes incremental updates through a rank-one perturbation, $\mathbf{x}_t \mathbf{x}_t^\top$, it is well-suited for the application of the Sherman-Morrison (SM) theorem [33]. The theorem represents an efficient method for updating the inverse of a matrix, declaring that if $\mathbf{A} \in \mathbb{R}^{n \times n}$ is an invertible square matrix with inverse \mathbf{A}^{-1} , and it undergoes a rank-one update $\mathbf{u} \mathbf{v}^\top$, with $\mathbf{u}, \mathbf{v} \in \mathbb{R}^n$, then the updated inverse can be efficiently computed by leveraging and updating the previous one, as demonstrated in (7).

$$(\mathbf{A} + \mathbf{u}\mathbf{v}^\top)^{-1} = \mathbf{A}^{-1} - \frac{\mathbf{A}^{-1}\mathbf{u}\mathbf{v}^\top\mathbf{A}^{-1}}{1 + \mathbf{v}^\top\mathbf{A}^{-1}\mathbf{u}} \quad (7)$$

The update rule in (2) modified with the Sherman-Morrison formula for the Disjoint algorithm is shown in (8), while Algorithm 1 presents the complete optimized algorithm.

$$\left(\mathbf{A}_{a_t} + \mathbf{x}_{t,a_t}\mathbf{x}_{t,a_t}^\top\right)^{-1} = \mathbf{A}_{a_t}^{-1} - \frac{\mathbf{A}_{a_t}^{-1}\mathbf{x}_{t,a_t}\mathbf{x}_{t,a_t}^\top\mathbf{A}_{a_t}^{-1}}{1 + \mathbf{x}_{t,a_t}^\top\mathbf{A}_{a_t}^{-1}\mathbf{x}_{t,a_t}} \quad (8)$$

This approach enables the direct storage of the inverse matrix \mathbf{A}_a^{-1} , reducing the stack memory requirements for intermediate variables, and completely eliminates the matrix inversion operation, significantly reducing the computational overhead by saving the inversion of $N[d \times d]$ matrices at each time step, at the cost of a minimal increase in the complexity of the update phase.

Fig. 1 illustrates the computational complexity trends of the Disjoint algorithm varying N and d parameters, comparing the standard and optimized versions. The proposed optimization reduces the asymptotic complexity of the Disjoint algorithm from $\mathcal{O}(d^3)$ to $\mathcal{O}(d^2)$.

Fig. 2 depicts the stack memory usage, obtained through a Python memory profiler, of both the traditional and optimized versions during the action selection and update phases, with d and N varying from 4 to 32. This approach

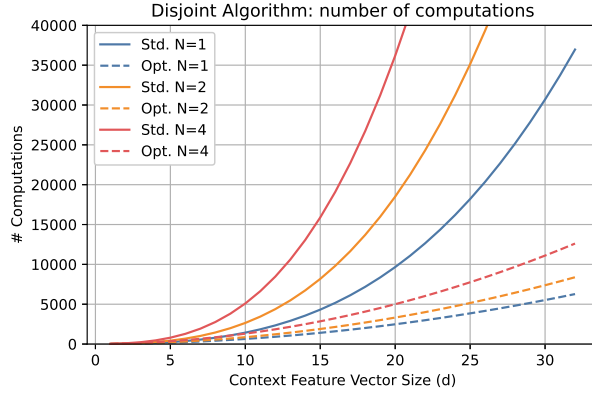


Fig. 1. Computational complexity trends for the standard Disjoint Algorithm and the proposed optimized version.

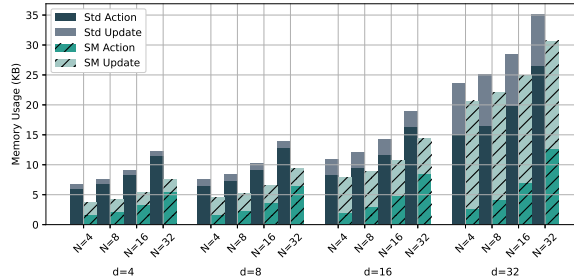


Fig. 2. Stack Memory Usage for the standard Disjoint Algorithm and the proposed optimized version.

reduces peak stack memory usage by up to 5 KB, making it feasible to run the algorithms on memory-constrained devices. This analysis also reveals that the optimization shifts stack memory usage from the action selection phase to the update one.

3.2 Optimization of the Hybrid LinearUCB through the Woodbury's Formula

In this section, the optimization strategies applied to the Disjoint algorithm are generalized and extended to the more complex Hybrid LinearUCB model.

Similar to the Disjoint variant, each action in the Hybrid algorithm is associated with a $d \times d$ matrix \mathbf{A}_a , used in its inverted form during the action selection phase and incrementally updated via rank-one perturbations, as per (5). Consequently, the Sherman-Morrison formula is again applicable, allowing to directly store \mathbf{A}_a^{-1} . However, although this approach improves computational efficiency by removing $N[d \times d]$ matrix inversions at each iteration, the overall performance gain for this model remains modest. The computational complexity is, in fact, predominantly driven by the inversion of the large $k \times k$ shared matrix, \mathbf{A}_0 . To illustrate, when considering $d = 8$ and $f = 16$, the inversion of \mathbf{A}_0 requires approximately 2,097,152 operations per iteration, which is significantly higher than the relatively minor cost of 512 operations for each \mathbf{A}_0 inversion. Consequently, it is crucial to explore whether a similar optimization strategy can be applied to \mathbf{A}_0 , aiming to substantially accelerate the algorithm.

The \mathbf{A}_0 matrix is always used in its inverted form during the action choice, and it is then incrementally updated according to (4) and (5), to which in the following we will refer as first and second update step, respectively.

In the first one, the Hybrid algorithm modifies \mathbf{A}_0 by incorporating the term $\mathbf{B}_{a_t}^\top \mathbf{A}_{a_t}^{-1} \mathbf{B}_{a_t}$, which represents a complex adjustment that goes beyond the normal rank-one perturbation, entailing the multiplication of three matrices. To efficiently address this more complex update scenario, we apply a generalized version of the Sherman-Morrison formula, known as the Woodbury matrix identity [22]. This formula is useful when the matrix update process involves an incremental rank- k perturbation. Given an invertible matrix $\mathbf{A} \in \mathbb{R}^{n \times n}$ with its inverse \mathbf{A}^{-1} , and matrices $\mathbf{U} \in \mathbb{R}^{n \times k}$, $\mathbf{C} \in \mathbb{R}^{k \times k}$, and $\mathbf{V} \in \mathbb{R}^{k \times n}$, the inverse of the updated matrix after applying a perturbation UCV can be computed by (9).

$$(\mathbf{A} + \mathbf{UCV})^{-1} = \mathbf{A}^{-1} - \mathbf{A}^{-1} \mathbf{U} (\mathbf{C}^{-1} + \mathbf{V} \mathbf{A}^{-1} \mathbf{U})^{-1} \mathbf{V} \mathbf{A}^{-1} \quad (9)$$

Applying the equation to the Hybrid algorithm makes it possible to modify the first update step as shown in (10).

$$\begin{aligned} (\mathbf{A}_0 + \mathbf{B}_{a_t}^\top \mathbf{A}_{a_t}^{-1} \mathbf{B}_{a_t})^{-1} &= \mathbf{A}_0^{-1} - \mathbf{A}_0^{-1} \mathbf{B}_{a_t}^\top \\ &\quad \cdot (\mathbf{A}_{a_t} + \mathbf{B}_{a_t} \mathbf{A}_0^{-1} \mathbf{B}_{a_t}^\top)^{-1} \mathbf{B}_{a_t} \mathbf{A}_0^{-1} \end{aligned} \quad (10)$$

Notably, \mathbf{A}_{a_t} required in this equation can be derived by inverting $\mathbf{A}_{a_t}^{-1}$, consistent with the traditional algorithm, where $\mathbf{A}_{a_t}^{-1}$ is calculated through inversion during the update phase.

The second update phase involves the sum of the outer product $\mathbf{z}_{t,a_t} \mathbf{z}_{t,a_t}^\top$ to \mathbf{A}_0 and the subtraction of $\mathbf{B}_{a_t}^\top \mathbf{A}_{a_t}^{-1} \mathbf{B}_{a_t}$.

The first sum involves a rank-one incremental update, since \mathbf{z}_{t,a_t} is a column vector in \mathbb{R}^k . Thus, this step can be efficiently handled using the Sherman-Morrison formula, as depicted in (11).

$$(\mathbf{A}_0 + \mathbf{z}_{t,a_t} \mathbf{z}_{t,a_t}^\top)^{-1} = \mathbf{A}_0^{-1} - \frac{\mathbf{A}_0^{-1} \mathbf{z}_{t,a_t} \mathbf{z}_{t,a_t}^\top \mathbf{A}_0^{-1}}{1 + \mathbf{z}_{t,a_t}^\top \mathbf{A}_0^{-1} \mathbf{z}_{t,a_t}} \quad (11)$$

Algorithm 2 optimized Hybrid LinearUCB

```

1: Input:  $\alpha \in \mathbb{R}_+$ 
2:  $\mathbf{A}_0^{-1} = \mathbf{I}_k$ 
3:  $\mathbf{b}_0 = \mathbf{0}_k$ 
4: for  $t = 1, 2, \dots, T$ 
5:   Observe the context for all arms  $a \in \mathcal{A}_t: (\mathbf{z}_{t,a}, \mathbf{x}_{t,a}) \in \mathbb{R}^{k+d}$ 
6:    $\hat{\boldsymbol{\beta}} = \mathbf{A}_0^{-1} \mathbf{b}_0$ 
7:   for all  $a \in \mathcal{A}_t$ 
8:     if  $t=1$ :
9:        $\mathbf{A}_a^{-1} = \mathbf{I}_d$ 
10:       $\mathbf{B}_a = \mathbf{0}_{d \times k}$ 
11:       $\mathbf{b}_a = \mathbf{0}_{d \times 1}$ 
12:     endif
13:      $\hat{\boldsymbol{\theta}}_a = \mathbf{A}_a^{-1} (\mathbf{b}_a - \mathbf{B}_a \hat{\boldsymbol{\beta}})$ 
14:      $s_{t,a} = \mathbf{z}_{t,a}^\top \mathbf{A}_0^{-1} \mathbf{z}_{t,a} - 2 \mathbf{z}_{t,a}^\top \mathbf{A}_0^{-1} \mathbf{B}_a^\top \mathbf{A}_a^{-1} \mathbf{x}_{t,a} +$ 
15:        $+ \mathbf{x}_{t,a}^\top \mathbf{A}_a^{-1} \mathbf{x}_{t,a} + \mathbf{x}_{t,a}^\top \mathbf{A}_a^{-1} \mathbf{B}_a \mathbf{A}_0^{-1} \mathbf{B}_a^\top \mathbf{A}_a^{-1} \mathbf{x}_{t,a}$ 
16:      $p_{t,a} = \mathbf{z}_{t,a}^\top \hat{\boldsymbol{\beta}} + \mathbf{x}_{t,a}^\top \hat{\boldsymbol{\theta}}_a + \alpha \sqrt{s_{t,a}}$ 
17:   endfor
18:   Choose  $a_t = \arg \max_{a \in \mathcal{A}_t} (p_{t,a})$ 
19:   and observe a real-valued payoff  $r_t$ 
20:    $\mathbf{A}_0^{-1} = \mathbf{A}_0^{-1} - \mathbf{A}_0^{-1} \mathbf{B}_{a_t}^\top (\mathbf{A}_{a_t} + \mathbf{B}_{a_t} \mathbf{A}_0^{-1} \mathbf{B}_{a_t}^\top)^{-1} \mathbf{B}_{a_t} \mathbf{A}_0^{-1}$ 
21:    $\mathbf{b}_0 = \mathbf{b}_0 + \mathbf{B}_{a_t}^\top \mathbf{A}_{a_t}^{-1} \mathbf{b}_{a_t}$ 
22:    $\mathbf{A}_{a_t}^{-1} = \mathbf{A}_{a_t}^{-1} - \frac{\mathbf{A}_{a_t}^{-1} \mathbf{x}_{t,a_t} \mathbf{x}_{t,a_t}^\top \mathbf{A}_{a_t}^{-1}}{1 + \mathbf{x}_{t,a_t}^\top \mathbf{A}_{a_t}^{-1} \mathbf{x}_{t,a_t}}$ 
23:    $\mathbf{B}_{a_t} = \mathbf{B}_{a_t} + \mathbf{x}_{t,a_t} \mathbf{z}_{t,a_t}^\top$ 
24:    $\mathbf{b}_{a_t} = \mathbf{b}_{a_t} + r_t \mathbf{x}_{t,a_t}$ 
25:    $\mathbf{A}_0^{-1} = \mathbf{A}_0^{-1} - \frac{\mathbf{A}_0^{-1} \mathbf{z}_{t,a_t} \mathbf{z}_{t,a_t}^\top \mathbf{A}_0^{-1}}{1 + \mathbf{z}_{t,a_t}^\top \mathbf{A}_0^{-1} \mathbf{z}_{t,a_t}}$ 
26:    $\mathbf{A}_0^{-1} = \mathbf{A}_0^{-1} + \mathbf{A}_0^{-1} \mathbf{B}_{a_t}^\top (\mathbf{A}_{a_t} - \mathbf{B}_{a_t} \mathbf{A}_0^{-1} \mathbf{B}_{a_t}^\top)^{-1} \mathbf{B}_{a_t} \mathbf{A}_0^{-1}$ 
27:    $\mathbf{b}_0 = \mathbf{b}_0 + r_t \mathbf{z}_{t,a_t} - \mathbf{B}_{a_t}^\top \mathbf{A}_{a_t}^{-1} \mathbf{b}_{a_t}$ 
28: endfor

```

The subtraction, instead, mirrors the mechanics of the first update step. The modified update rule is shown in (12).

$$\begin{aligned}
(\mathbf{A}_0 - \mathbf{B}_{a_t}^\top \mathbf{A}_{a_t}^{-1} \mathbf{B}_{a_t})^{-1} &= \mathbf{A}_0^{-1} + \mathbf{A}_0^{-1} \mathbf{B}_{a_t}^\top \cdot \\
&\cdot (\mathbf{A}_{a_t} - \mathbf{B}_{a_t} \mathbf{A}_0^{-1} \mathbf{B}_{a_t}^\top)^{-1} \mathbf{B}_{a_t} \mathbf{A}_0^{-1}
\end{aligned} \tag{12}$$

Algorithm 2 presents the optimized Hybrid algorithm. As depicted, this approach only involves the \mathbf{A}_0^{-1} and \mathbf{A}_a^{-1} matrices, updating them using the Sherman-Morrison-Woodbury (SMW) formulas. This enables the direct storage of the inverse matrices and reduces the number of matrix inversions from N inversions of $[d \times d]$ matrices and one inversion of a $k \times k$ matrix per iteration to a constant $3[d \times d]$ inversions per iteration in the update process. This notably decreases computational complexity by removing the need for the large $k \times k$ inversion and eliminating the dependency on N .

Fig. 3 depicts the computational complexity trends of the Hybrid algorithm with a constant $N = 8$, while varying f , and d , contrasting the standard and optimized versions. Overall, the optimization leads to an asymptotic computational complexity of $O(k^2 d)$ or $O(f^2 d^3)$ instead of the larger $O(k^3)$ or $O(f^3 d^3)$. These results also illustrate the relative

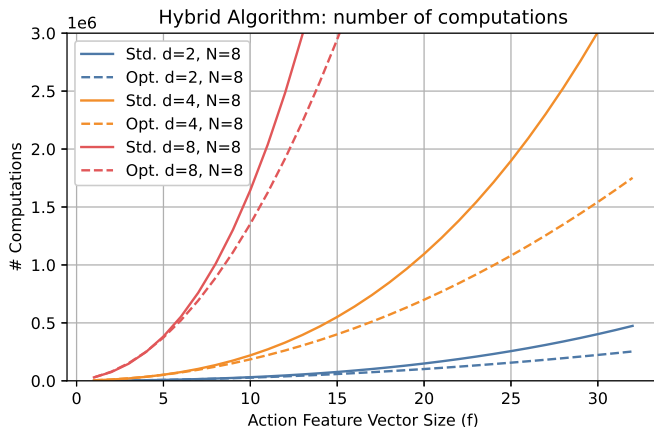


Fig. 3. Computational complexity trends for the standard Hybrid Algorithm and the proposed optimized version.

Table 1. Asymptotic computational complexity in the original Disjoint and Hybrid Algorithms and in the proposed optimized versions

	Disjoint LinearUCB		Hybrid LinearUCB	
	Stage 1	Stage 2	Stage 1	Stage 2
Standard	$O(d^3)$	$O(d^2)$	$O(k^3)$	$O(k^2d)$
Optimized	$O(d^2)$	$O(d^2)$	$O(k^2d)$	$O(k^2d)$

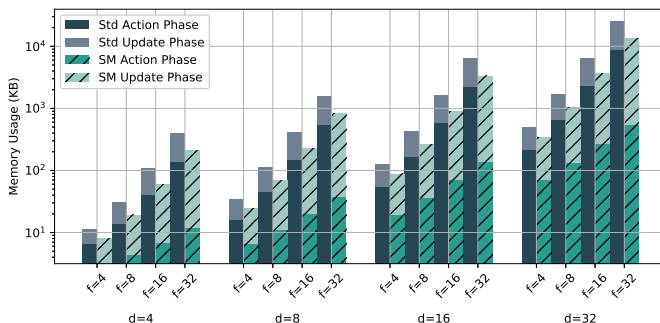


Fig. 4. Stack Memory Usage for the standard Hybrid Algorithm and the proposed optimized version.

complexity of the Hybrid algorithm compared to the Disjoint variant, showing how rapidly the computational demands escalate with increasing problem parameters.

Table 1 summarizes the impact of the proposed algorithmic optimizations on the computational complexity of the algorithms, both during the action selection and update processes (Stage 1 and Stage 2).

Fig. 4 shows the stack memory usage of the hybrid algorithm, measured using a Python memory profiler, with the d and f parameters varying from 4 to 32. The proposed optimization reduces peak memory usage by up to 12 KB.

3.3 Stability and Round-off Errors

In the previous section, we demonstrated how the Sherman–Morrison–Woodbury formula can significantly reduce the computational cost of the LinearUCB algorithm by avoiding complex and time-consuming matrix inversions. However, while this formula offers an exact solution for updating matrix inverses, its practical application can be affected by round-off errors due to finite-precision arithmetic, potentially leading to instabilities when the matrix becomes ill-conditioned. In this section, we first establish the stability of the proposed approach by demonstrating that the inverse covariance matrices in the LinearUCB algorithms remain well-conditioned and stable over time. We then investigate the impact of round-off errors as the number of iterations grows, using synthetic datasets to quantify error accumulation. Finally, we present a novel strategy to mitigate these errors in scenarios where high precision is critical. We begin our analysis with the Disjoint LinearUCB algorithm, addressing its simpler structure, and then we extend our findings to the more complex Hybrid one.

3.3.1 Stability of the Covariance Matrices. Round-off or rounding errors arise from the finite-precision arithmetic inherent in digital computations and can accumulate over successive operations, potentially leading to numerical inaccuracies. When recomputing the inverse of a matrix from scratch after each modification, each inversion is independent of previous computations, making this approach generally more resilient to the accumulation of round-off errors. In contrast, in incremental update mechanisms, small errors can accumulate across iterations, which may gradually lead to noticeable inaccuracies. In detail, in the SM formula, round-off errors are prone to amplification and can introduce instabilities in two main scenarios:

- (1) Denominator Approaching Zero: The SM formula contains a denominator term that, when approaching zero, can render the update unstable. This scenario can lead to large numerical errors or even division by zero, resulting in computational failures.
- (2) Singular or Ill-Conditioned Inverse Matrices: If the inverse matrix becomes singular or ill-conditioned the calculations may amplify numerical errors. An ill-conditioned matrix is highly sensitive to minor perturbations, which can result in substantial deviations in the output, thereby compromising the algorithm’s stability.

To ensure the stability of the SM update in our optimized LinearUCB algorithms, in this section we demonstrate that these two conditions are avoided. To do that, is sufficient to show that the involved covariance matrices \mathbf{A}_{a_t} remain positive and definite throughout the iterations [30]. This is due to two key reasons:

- (1) If \mathbf{A}_{a_t} is positive definite, then the updated matrix $\mathbf{A}_{a_{t+1}} = \mathbf{A}_{a_t} + \mathbf{x}_t \mathbf{x}_t^\top$ and its inverse $\mathbf{A}_{a_{t+1}}^{-1}$ are also positive definite ensuring that the condition number of \mathbf{A}_{a_t} remains bounded, preventing the matrix from becoming ill-conditioned. In fact, if \mathbf{A}_{a_t} is positive definite at iteration t , since $\mathbf{x}_t \mathbf{x}_t^\top$ is positive semi-definite for any non-zero \mathbf{x}_t , the sum of a positive definite matrix \mathbf{A}_{a_t} and a positive semi-definite matrix $\mathbf{x}_t \mathbf{x}_t^\top$ remains positive definite.
- (2) if the matrix is positive definite, the denominator in the Sherman-Morrison formula, $d_t = 1 + \mathbf{x}_t^\top \mathbf{A}_{a_t}^{-1} \mathbf{x}_t$, is always strictly greater than one. In fact, since $\mathbf{A}_{a_t}^{-1}$ is positive definite (as proven in the previous step), for any non-zero \mathbf{x}_t , we have $\mathbf{x}_t^\top \mathbf{A}_{a_t}^{-1} \mathbf{x}_t > 0$. Therefore, the denominator $d_t = 1 + \mathbf{x}_t^\top \mathbf{A}_{a_t}^{-1} \mathbf{x}_t > 1$.

In the optimized Disjoint LinearUCB algorithm proposed in Algorithm 1, the inverse covariance matrices \mathbf{A}_a^{-1} are positive definite by construction, as they are initialized as $\mathbf{A}_a = \lambda \mathbf{I}_d$ at time-step $t = 0$, where $\lambda > 0$ is the regularization parameter and \mathbf{I}_d is the $d \times d$ identity matrix. From what we demonstrated, this implies that the denominator in the SM formula remains greater than one and that these matrices remain positive definite and well-conditioned throughout

the iterations. As a result, round-off errors are not amplified, and the algorithm is expected to maintain numerical stability over time.

The same analysis extends to the more complex optimized Hybrid LinearUCB algorithm presented in Algorithm 2, which incorporates global features shared across all arms. We already proved that each \mathbf{A}_{a_t} matrix remains positive definite after the update phase; for the Hybrid case, we now demonstrate the same for the global covariance matrix \mathbf{A}_0 and its update. At time-step $t = 0$, \mathbf{A}_0 is initialized as $\lambda \mathbf{I}_k$, where $\lambda > 0$ and \mathbf{I}_k is the $k \times k$ identity matrix. At each iteration t , \mathbf{A}_0 is updated when an arm a_t is selected according to (4) and (5). In (4), $\mathbf{z}_{t,a_t} \mathbf{z}_{t,a_t}^\top$ is positive semi-definite (as it is an outer product of a vector with itself), and thus, adding it to the positive definite \mathbf{A}_0 results in a positive definite matrix. The resulting matrix is further updated with the term $\mathbf{B}_{a_t}^\top \mathbf{A}_{a_t}^{-1} \mathbf{B}_{a_t}$ in (5). To show that this term is positive semi-definite, we need to demonstrate that for any vector \mathbf{x} ,

$$\mathbf{x}^\top (\mathbf{B}_{a_t}^\top \mathbf{A}_{a_t}^{-1} \mathbf{B}_{a_t}) \mathbf{x} \geq 0.$$

However, since we already demonstrated that the matrix $\mathbf{A}_{a_t}^{-1}$ is positive definite, we know that for any non-zero vector \mathbf{y} , $\mathbf{y}^\top \mathbf{A}_{a_t}^{-1} \mathbf{y} > 0$. Setting $\mathbf{y} = \mathbf{B}_{a_t} \mathbf{x}$ gives:

$$\mathbf{x}^\top \mathbf{B}_{a_t} \mathbf{A}_{a_t}^{-1} \mathbf{B}_{a_t}^\top \mathbf{x} = \mathbf{y}^\top \mathbf{A}_{a_t}^{-1} \mathbf{y} \geq 0.$$

This confirms that $\mathbf{B}_{a_t} \mathbf{A}_{a_t}^{-1} \mathbf{B}_{a_t}^\top$ is positive semi-definite, and therefore, \mathbf{A}_0 remains positive definite.

Consequently, both the global and arm-specific covariance matrices in the Hybrid algorithm remain positive definite over time.

By proving that the matrices of the algorithms are positive definite, we ensure that their inverses are also positive definite and well-conditioned. This positive definiteness of the inverses is crucial for maintaining numerical stability in the SMW updates, as it prevents the amplification of round-off errors and ensures the robustness of the algorithms over time. Thus, the optimized LinearUCB algorithm is robust against numerical issues associated with finite-precision arithmetic.

3.3.2 Assessing the Accumulation of Round-Off Errors. In the previous section, we demonstrated that the covariance matrices within the LinearUCB algorithms remain well-conditioned throughout the iterations, making them suitable candidates for the Sherman–Morrison update. This condition prevents the amplification of round-off errors over time, allowing the incremental update approach in the optimized LinearUCB algorithms to maintain numerical stability effectively.

To further evaluate the practical impact of round-off errors, we conducted an empirical assessment. We ran 100,000 iterations on synthetic datasets for both the Disjoint and Hybrid LinearUCB algorithms. At each iteration, we compared the matrices $\mathbf{A}_{a_t}^{-1}$ and \mathbf{A}_0^{-1} obtained through incremental updates with those obtained via the traditional full matrix inversion approach. Figures 5 and 6 display the error growth, computed as the Frobenius norm of the difference between matrices, and the average reward for both the Disjoint and Hybrid LinearUCB algorithms.

For the Disjoint algorithm, the total difference measured using the Frobenius norm, consistently hovers around 1×10^{-15} , indicating that round-off errors accumulate very slowly and remain completely negligible even after 100,000 iterations.

In contrast, in the Hybrid Linear UCB algorithm, we observed a larger accumulation of round-off errors, particularly in the global matrix \mathbf{A}_0 , where the error grew up to 1×10^{-4} after 100,000 iterations. This larger accumulation is primarily

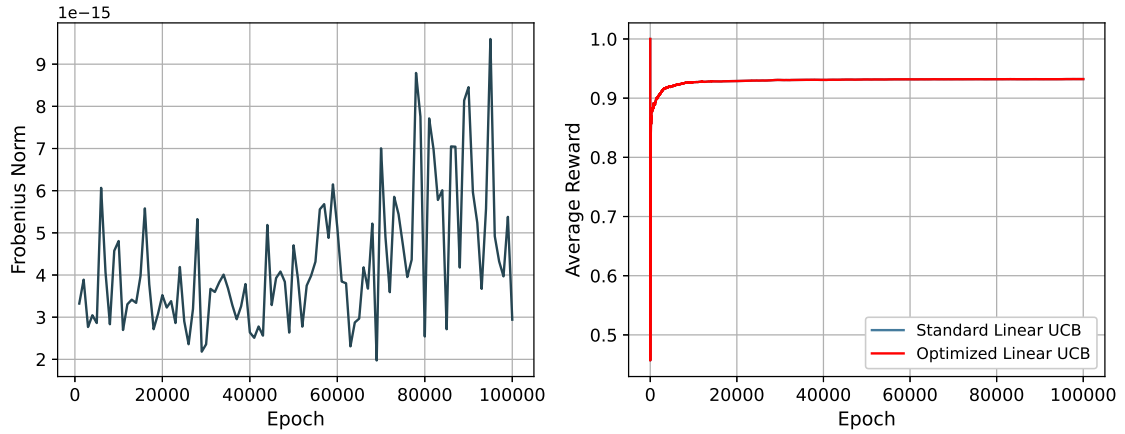


Fig. 5. Error growth in the Disjoint Linear UCB algorithm, measured by the Frobenius norm of the difference between $\mathbf{A}_{a_t}^{-1}$ (computed incrementally) and the same matrix obtained via full inversion.

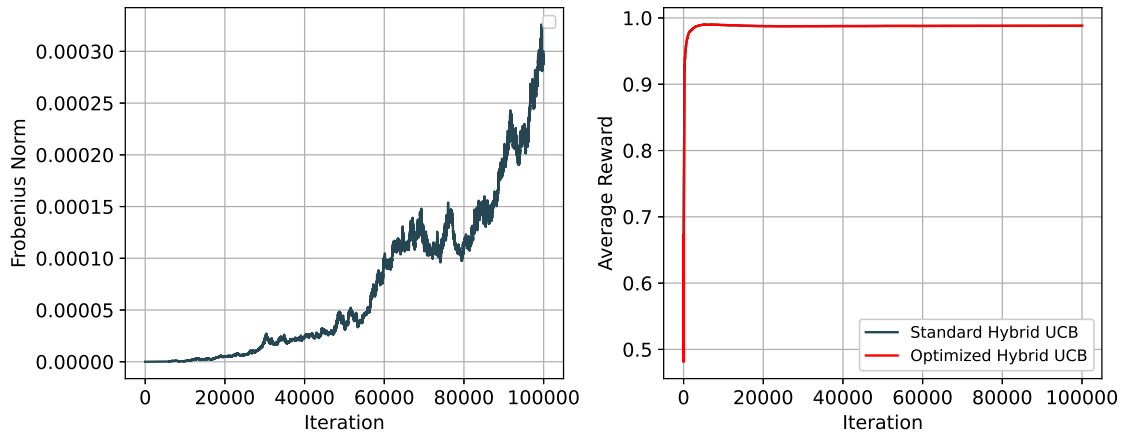


Fig. 6. Error growth in the Hybrid Linear UCB algorithm, measured by the Frobenius norm of the difference between \mathbf{A}_0^{-1} (computed incrementally) and the same matrix obtained via full inversion.

due to the fact that while the arm-specific matrices \mathbf{A}_a are updated only when a particular arm is selected, the global matrix \mathbf{A}_0 is updated at every iteration, making it more prone to round-off error accumulation.

An important observation is that in both algorithms, the optimization introduced by the Sherman-Morrison-Woodbury approach had no effect on the decision-making process. Across 100,000 iterations, the actions selected by the optimized methods were identical to those chosen by the traditional matrix inversion, resulting in the same cumulative reward for both approaches. This suggests that the round-off errors introduced by the incremental updates had a negligible impact on the algorithm's performance, even after a substantial number of iterations.

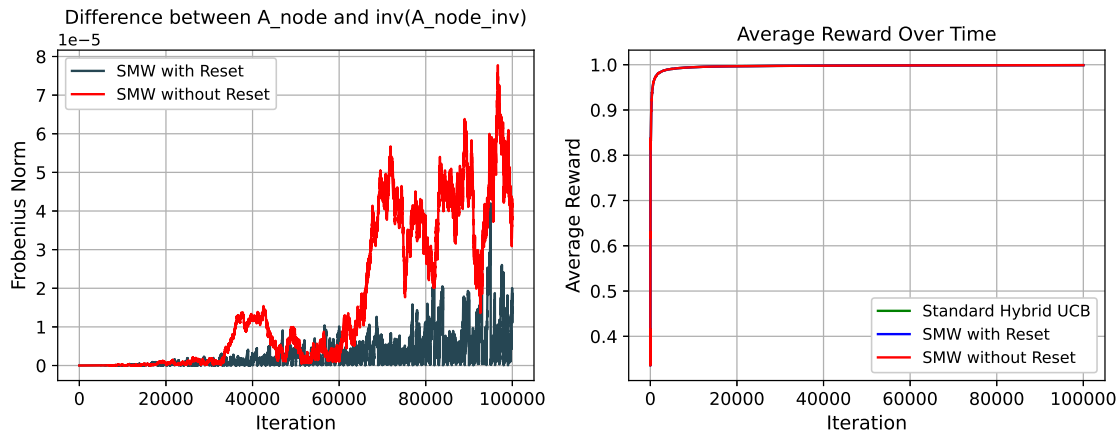


Fig. 7. Error growth in the Hybrid Linear UCB algorithm with periodic correction of the inverse matrices (every 5000 iterations).

3.3.3 Proposed Solution to Mitigate Round-Off Errors. While our results show that the round-off errors in the optimized SMW approach have negligible impact on performance, in certain applications where the algorithm may be run for an extremely high number of iterations, it could be important to mitigate the accumulation of these errors. To address this, we propose a method to periodically correct the inverse matrices, thus alleviating the influence of round-off errors over time. This approach consists of periodically replacing or correcting the inverse matrices A_a^{-1} and A_0^{-1} . When memory constraints are not a major issue, we can store both the direct matrices A_a and A_0 , as well as their inverses. The direct matrices are updated in each iteration using the traditional algorithmic formulation (i.e., without incremental updates), while the inverse matrices are incrementally updated via the SMW approach and used for action selection. Every N iterations, where N is a tunable integer, the inverse matrices A_a^{-1} and A_0^{-1} are replaced by the exact inverses computed from their corresponding direct matrices. This periodic correction reduces the impact of round-off errors without requiring matrix inversion at every step, thus maintaining the computational efficiency of the SMW approach. The trade-off here is between the complexity of periodically computing matrix inversions and the degree to which round-off errors are mitigated. The value of N can be adjusted depending on the specific application requirements, balancing between minimizing error growth and minimizing the overhead introduced by performing full matrix inversions.

To demonstrate the effectiveness of this approach, we implemented this mechanism in the Hybrid Linear UCB algorithm and ran it for 100,000 iterations with $N = 5000$. The results, shown in Figure 7, indicate that the total round-off error can be reduced by up to two orders of magnitude compared to the original uncorrected approach.

This periodic correction approach provides a solution for applications where the algorithm is expected to run for an extremely high number of iterations, and the accumulation of round-off errors could eventually affect performance. By only computing full matrix inversions every N iterations, this method strikes a balance between computational efficiency and numerical precision. However, it introduces additional memory requirements and complexity. Notably, the overall computational load remains significantly reduced compared to traditional approaches, as matrix inversion is performed only once every N iterations, as opposed to every iteration. The value of N thus provides a flexible parameter to trade off between complexity and round-off error mitigation.

4 Vector Computing Acceleration

Vector hardware accelerators are specialized computing units designed to efficiently process operations on vectors of numbers, exploiting data-level parallelism [19]. While vector processors have been traditionally employed in supercomputers, there is an evident trend in adopting vector computing support in embedded processing systems [8, 24]. Given the strong dependence of LinearUCB algorithms on matrix operations, discussed in Sections 2 and 3, this Section explores if and how vector computing architectural support may be harnessed to improve the algorithm execution time by implementing fundamental matrix operations in terms of elementary operations on vectors.

4.1 Reference Embedded Vector Computing Platform

For the purpose of our study, without loss of generality we adopted the Klessydra embedded processor family [8, 9, 15] to explore the impact of vector computing acceleration on the execution of the proposed algorithm. Klessydra processors are compliant with the open RISC-V instruction set architecture and are fully compatible with the PULPino open-source System-on-Chip platform.

The Klessydra-T13 core features a Vector Computing Unit (VCU) developed as a configurable hardware accelerator specifically designed for vector operations. The unit is equipped with dedicated local data storage referred to as Scratchpad Memories (SPMs) and can be configured at synthesis-time in terms of the SIMD (Single Instruction Multiple Data), which defines the number of vector elements processed in parallel. A custom RISC-V-compliant instruction set extension, integrated in the RISC-V GCC compiler tool-chain, facilitates the programmer’s access to the VCU by exposing elementary vector arithmetic operations as intrinsic function calls. The vector size is dynamically specified at runtime using a dedicated Current Status Register. The VCU leverages a hardware loop mechanism to efficiently repeat the required instruction until all vector elements are processed—based on the configured SIMD and vector size—without requiring additional instruction fetches. The vector operations used for matrix-related computations in the algorithms of the proposed study are reported in the following section.

To implement and execute LinearUCB algorithms on the Klessydra-T13 embedded processor, constrained by lack of dynamic memory allocation and of floating-point support, we developed a versatile custom C++ library based on static allocation and fixed-point data representation. In order to quantify the impact of vector computing support on the final performance, the library was designed to process matrix operations in two distinct modes: a software-only mode, compiled on the standard RISC-V instruction set executed by the scalar processing core, and one vectorized version utilizing the VCU support. In the vectorized version, each arithmetic matrix operation was meticulously parallelized using the specialized vector intrinsic functions supported by the compiler toolchain.

4.2 Mapping LinearUCB algorithms on the vector accelerator

The application of the VCU specialized functions to Algorithms 1 and 2 is detailed below.

- matrix addition: this algorithm step was encoded using the *kaddv (rd), (rs1), (rs2)* instruction, which allows the addition of two vectors located in the SPMs in a SIMD fashion. Executing this operation for each row, reduces the matrix addition time by a factor equal to the number of parallel functional units in the VCU.
- matrix multiplication: this algorithm step was encoded using the *kvmulpsrf (rd), (rs1), (rs2)* instruction that performs a fixed-point multiplication between a vector from the scratchpad memory and a scalar from the register file. We used an iterative approach in which an entire row of the first matrix is multiplied by a scalar element from a second row. This produces intermediate products, which are accumulated across vector lanes to

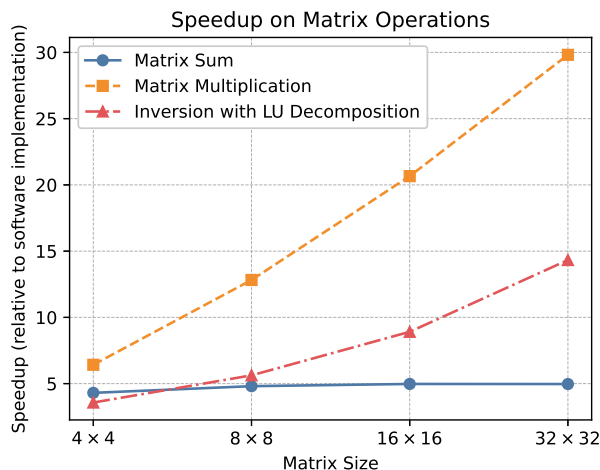


Fig. 8. Speedup attained by the Klessydra-T13 vector computing acceleration on the fundamental matrix computation kernels used in LinearUCB algorithms

form the corresponding row elements of the resultant matrix. By repeating this process for each row, the ability to perform multiple vector-scalar multiplications in a single cycle is fully leveraged, significantly enhancing the operation speed. The vector-scalar product is executed in hardware in double integer precision, and the resulting product is subsequently right-shifted by the appropriate scaling factor to maintain the output data width.

- matrix inversion: this algorithm step was implemented by applying the LU factorization technique, which was encoded exploiting the *kvdiv (rd), (rs1), (rs2)* instruction for executing element-wise vector divisions [4] leveraging the variable latency dividers integrated in the VCU [3].

Figure 8 presents the performance gains achieved for the above discussed matrix operations, using a SIMD equal to 4. The speedup metric was chosen as the ratio between the clock cycles required by the standard operation (i.e. compiled for the RISC-V instruction set and executed on the Klessydra-T13 processor without vector computing support) and the cycles required by the accelerated operation (i.e. compiled on the extended instruction set exploiting the vector computing support of the Klessydra-T13 core). The speedup result is analyzed across different matrix sizes. The matrix addition exhibits maximum benefit from parallel processing, demonstrating a consistent speedup across all matrix sizes, equivalent to a factor of 4×. Matrix multiplication displays a different speedup pattern as the matrix size grows. The adopted parallel approach reaches a speed up equal to 6.42× in the case of 4 × 4 matrices, which scales up to 29.82× for 32 × 32. The speedup factor greater than the SIMD amount is explained by the heavy memory access overhead suffered in the standard scalar execution. The inversion operation represents the most challenging operation to be parallelized owing to its inherently sequential nature. Nevertheless, utilizing LU matrix factorization techniques and the optimized dividers in the VCU allows a notable acceleration of up to 15× for 32 × 32 matrices.

5 Results on full algorithm execution

This section analyzes the cumulative impact of the proposed dual optimization strategy on the LinearUCB algorithms implemented and executed on embedded processor platforms. The purpose of the reported performance data is to

contextualize the results obtainable with algorithmic enhancement and explicit vectorization in the low-end embedded system domain. For this reason, we chose the Cortex M4 STM32 Nucleo board, the Cortex A72 Raspberry PI 4 Model B board, and the Klessydra T13 PULPino open-source soft-processor equipped with basic vector acceleration. The contextualization of the results does not aim to demonstrate absolute superior performance to specific commercial products, yet to give evidence of the effectiveness of the explored techniques in limited hardware resource scenarios.

For the Disjoint algorithm, we varied the size of the context feature vector (d) from 4 to 32, while keeping N equal to 8. For the hybrid algorithm, we varied the size of the action feature vector (f) from 4 to 32, keeping d and N equal to 8. The following subsections describe the adopted methodology in detail and discuss the obtained results in terms of execution time and energy consumption.

5.1 Methodology

The standard software C++ implementation and the optimized version of both the Disjoint and Hybrid LinearUCB algorithms were compiled for the PULPino platform, the STM32 platform, and the Raspberry PI 4 platform. The compilation for PULPino Klessydra T13 was done for no vector computing support and for a SIMD = 4 vector acceleration support. This SIMD width was selected as it offers a balance between performance and area, making it well-suited for embedded applications [15]. The Klessydra PULPino platform was implemented on the Xilinx Vivado tool suite targeting the Kintex-7 KC705 FPGA device (xc7k325tffg900-2), with a target clock frequency of 100 MHz. The synthesis reported no timing violations.

Execution time estimations were done by direct execution on the STM32 and Raspberry boards, while they were done by cycle-accurate RTL simulation on QuestaSim for the Klessydra T13 implementations, with 100 MHz simulated clock frequency. The speedup factor was calculated as the ratio between the execution times of the traditional algorithm and the optimized algorithm.

For energy consumption estimation, we measured the power absorbed by the STM32 and Raspberry Pi boards during algorithm execution using a power supply with integrated power measurement capabilities. The instrument, connected to an AC source and supplying the target boards with DC power, continuously monitored the absorbed current. After synchronizing with a digital trigger signal from the target boards, the average power consumption was recorded during algorithm execution. For the Klessydra T13 implementations, we extracted the post-implementation netlist and conducted gate-level simulations of the algorithms. The simulations provided the switching activity *.saif* files, which were processed by the Vivado power estimator to assess the dynamic power ($P_{dynamic}$) of the core. For all of the Klessydra, Cortex A71 and Cortex M4 processors, the energy consumption was considered for the core and the memories only, excluding all the peripherals. For all the processors, we calculated the total energy consumption as the average power consumption multiplied by the execution time. The energy reduction factor was then calculated as the ratio between dynamic energy consumptions of the optimized algorithm and the traditional algorithm.

Tables 2 and 3 summarize all the obtained results for the Disjoint and Hybrid algorithms, on the chosen embedded execution platforms. The analysis of the specific impact of each optimization step is reported in the following.

5.2 Algorithmic optimization impact on execution time

Efficient execution time is essential for deploying AI algorithms in applications with stringent real-time requirements. Figure 9a illustrates the impact of the Sherman-Morrison algorithmic optimization on the Disjoint LinearUCB algorithm with N equal to 8. Varying the context feature vector size (d) from 4 to 32 the proposed approach achieves a speed up that ranges from 5.04× to 25.73× on Klessydra T13, from 3.19× to 22.84× on Cortex M4 and from 4.13× to 29.91×

Table 2. Performance results for the Disjoint Algorithm in the Std. and Opt. versions on the examined execution platforms

	d	Cortex M4 STM32 Nucleo		Cortex A72 Raspberry PI 4		Klessydra T13 PULPino			
		Std.	Opt.	Std.	Opt.	Std.	Opt.	Std. with VCU	Opt. with VCU
Cycle count	4	433024	135586	198000	48000	96117	19078	27905	13371
	8	2523904	467402	1117500	141000	484456	52767	131972	28854
	16	19694862	1677126	7629000	487500	2734595	181357	498280	86287
	32	148464048	6499592	55540500	1857000	17562142	682584	2017706	304447
Execution time [μs]	4	5412	1695	132	32	961	190	279	134
	8	31548	5843	745	94	4844	527	1320	289
	16	246185	20964	5086	325	27345	1813	4983	863
	32	1855800	81244	37027	1238	175621	6825	20177	3044
Energy cons. [μJ]	4	838	262	435	105	185	40	54	27
	8	4890	905	2458	310	939	113	259	59
	16	38158	3249	16783	1072	5387	397	986	179
	32	287649	12592	122189	4085	35651	1549	4095	645

Table 3. Performance results for the Hybrid Algorithm in the Std. and Opt. versions on the examined execution platforms

	f	Cortex M4 STM32 Nucleo		Cortex A72 RASpberry PI 4		Klessydra T13 PULPino			
		Std.	Opt.	Std.	Opt.	Std.	Opt.	Std. with VCU	Opt. with VCU
Cycle count	4	5751676	4355380	2325000	1785000	1029600	909378	413274	327463
	8	28419702	14498906	11142000	5679000	4594114	2919300	1307512	974813
	16	176841698	52908188	67779000	20509500	26216770	10454626	4741130	3338271
	32	N.A.	N.A.	456472500	78625500	176168851	39638697	19156387	12768900
Execution time [μs]	4	71895	54442	1550	1190	10296	9093	4133	3275
	8	355246	181236	7428	3786	45941	29193	13075	9748
	16	2210521	661352	45186	13673	262167	104546	47411	33383
	32	N.A.	N.A.	304315	52417	1761688	396487	191564	127689
Energy cons. [μJ]	4	11143	8438	5115	3927	1945	1746	847	677
	8	55063	28091	24512	12493	8912	5634	2706	2037
	16	342630	102509	149113	45120	53482	20700	10193	7344
	32	N.A.	N.A.	1004239	172976	389333	80466	43676	30006

on Cortex A72. The observed linear increase in speedup with d aligns with the theoretical reduction in complexity from $O(d^3)$ to $O(d^2)$ described in Table 1 and Fig. 1. These results highlights how the removed matrix inversions constitute the performance bottleneck of the algorithm and strongly limits its scalability. Notably, as described in Section 3, increasing the number of actions, N , would further enhance the speedup provided by the algorithmic optimization.

The same analysis on the execution time is depicted in Figure 9b for the Hybrid algorithm, varying the action vector size (f) from 4 to 32, while keeping d and N equal to 8. The algorithmic optimization based on the Sherman-Morrison-Woodbury formulas results in speedups ranging from 1.13 \times to 4.45 \times on the Klessydra-T13 core, and from 1.30 \times to 5.80 \times on the Cortex-A7. For the Cortex-M4 core, the speedup increases from 1.32 \times at $f = 4$ to 3.34 \times at $f = 16$. Notably, data for $f = 32$ are absent due to the memory demands of this configuration, which exceed the capabilities of the target Nucleo Board. The results demonstrate a linear increase in speedup with f , consistent with the theoretical reduction in complexity from $O(f^3 d^3)$ to $O(f^2 d^3)$, as outlined in Table 1 and Fig. 3. As detailed in Figure 3, increasing the value of d would increase the speedup for the optimized Hybrid algorithm, whereas increasing N has a minimal impact on performance due to the dominance of arithmetic operations on the complex $k \times k$ shared matrix.

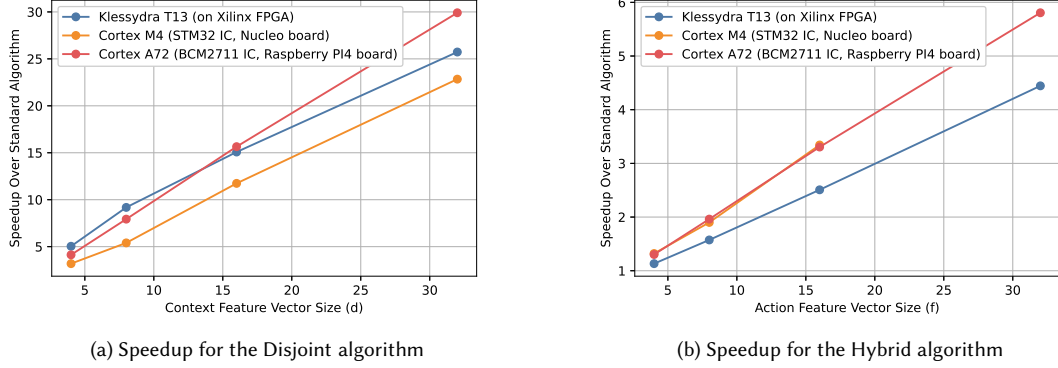


Fig. 9. Algorithmic optimization impact on execution time

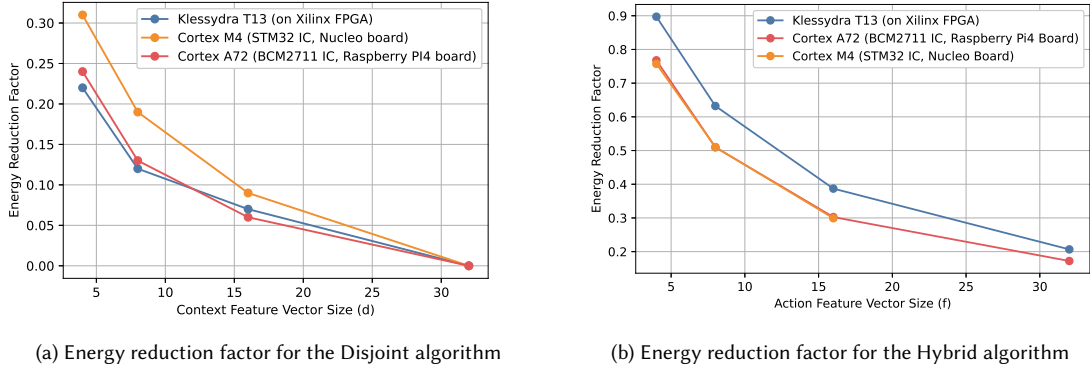


Fig. 10. Algorithmic optimization impact on energy consumption

5.3 Algorithmic optimization impact on energy consumption

Energy consumption is another critical factor when deploying AI algorithms in low-power environments. This section examines how the proposed algorithmic optimizations enhance the energy efficiency of the LinearUCB algorithms.

Figure 10a depicts the results obtained for the Disjoint algorithm varying the context feature vector size (d) while keeping N equal to 8. As already observed for the execution time, as d increases, so does the advantage brought by algorithmic optimizations. The energy reduction factor decreases asymptotically as the ratio $\frac{O(d^2)}{O(d^3)} \propto \frac{1}{d}$, aligning with the theoretical analysis of the computational complexity presented in Table 1 and Fig.1. On the Klessydra-T13 core, the energy reduction factors ranges from 0.22, to 0.04 when d is equal to 4 and 32, respectively. A similar pattern in energy efficiency can be observed for the Cortex-M4 and Cortex-M7 platforms, with energy reduction factors ranging from 0.31 to 0.04 and from 0.24 to 0.03, respectively.

For the Hybrid algorithm the energy reduction obtained by the algorithmic optimization is shown in Figure 10b varying the action feature vector size (f) from 4 to 32, while keeping d and N equal to 8. The trend shows an asymptotic decrease as the ratio $\frac{O(f^2 d^3)}{O(f^3 d^3)} \propto \frac{1}{f}$, as outlined in Table 1 and Fig. 3. On Klessydra, the energy reduction decreases from

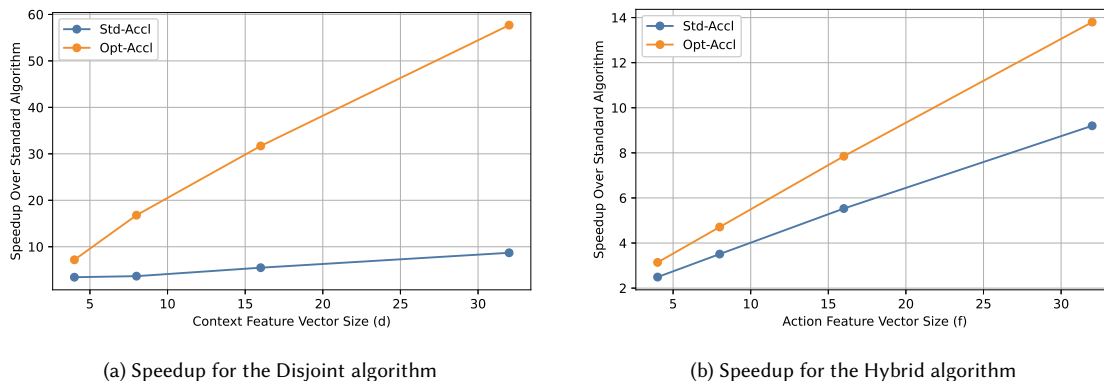


Fig. 11. Vector computing acceleration impact on execution time

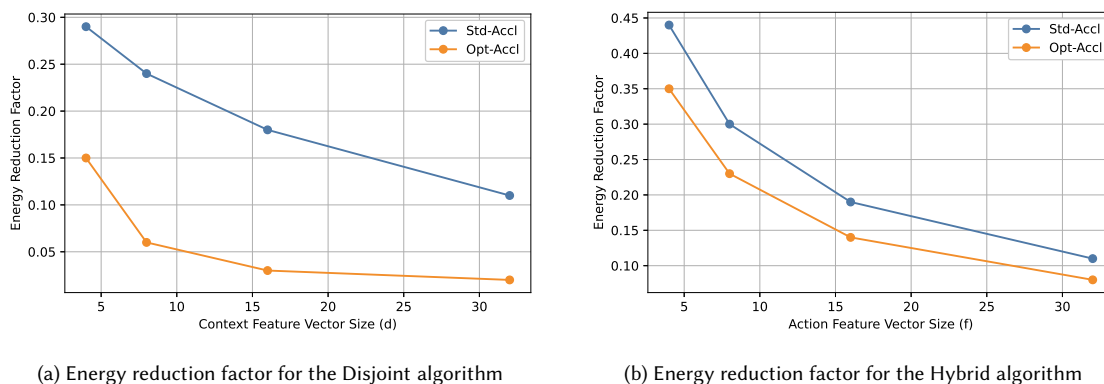


Fig. 12. Vector computing acceleration impact on energy consumption

0.89 to 0.20. As already discussed for the execution time, the data for $f = 32$ with Cortex-M4 are not present due to the high memory demands of this configuration, but the trend for this platform closely follows the one obtained for the Cortex-A72, in which the energy reduction factor ranges from 0.76 to 0.17.

5.4 Vector computing acceleration impact on execution time

The impact of vector computing support on the LinearUCB algorithms was evaluated by executing both the standard and optimized versions on the Klessydra-T13 core, utilizing the VCU support for accelerating the basic matrix operations, as detailed in Section 4. The execution times have been measured and compared with the ones obtained by software executions and the results in terms of speedup are reported in Figures 11a and 11b for the Disjoint and Hybrid algorithms, respectively.

In the Disjoint version, vector computing acceleration achieves speedups ranging from $3.44\times$ at $d = 4$ to $8.70\times$ at $d = 32$ for the standard version. When combined with algorithmic optimizations, these speedups escalated dramatically ranging from $7.18\times$ to $57.68\times$.

For the Hybrid algorithm, the vector computing acceleration applied to the standard version of the algorithm results in speedups ranging from 2.49 \times when $f = 4$ to 9.19 \times at $f = 32$. When vector acceleration and algorithmic optimization are synergically applied, the speedup ranges from 3.15 \times to 13.82 \times , resulting in essential improvement for deploying complex algorithms like the Hybrid one on embedded systems.

Notably, the observed trends for the accelerated standard versions confirm the expected linear speedup provided by vector support when varying the matrix size observed in Fig.8. Since both the algorithmic optimization and the vector acceleration independently contribute linear scaling properties, their combination results in an overall effect on speedup that remains linear but with a greater magnitude.

5.5 Vector computing acceleration impact on energy consumption

Finally, the impact of vector computing support on the energy consumption of the target algorithms is depicted in Figures 12a and 12b. For the standard Disjoint algorithm, the energy reduction factor decreases from 0.29 to 0.11 as d is increased from 4 to 32. The optimized version further reduces these values from 0.15 to 0.02.

The effect of vector acceleration is even more pronounced in the Hybrid algorithm, where the energy reduction factor ranges from 0.44 to 0.11 for the standard version and from 0.35 to 0.08 for the optimized one.

The observed reductions align with theoretical expectations of an inverse relationship with d and f due to the linear scaling properties of vector acceleration when varying matrix sizes, as demonstrated in Fig. 8.

5.6 Discussion

Overall, the obtained results demonstrate the effectiveness of the dual-pronged optimization strategy, which combines algorithmic improvements with vector processing support to reduce execution time and energy consumption, enabling faster and more power efficient application of LinearUCB algorithms in embedded learning systems. For the Disjoint algorithm, the algorithmic refinements based on the Sherman-Morrison formula replace heavy matrix inversions with lightweight incremental updates, resulting in significant execution time improvements across all platforms, with a maximum speedup on Klessydra equal to 25.73 \times . At the same time, although less effective in this case, vector computing support achieves a maximum speedup of 8.70 \times . Combined, the total speedup reaches 58 \times . A different trend can be observed for the Hybrid algorithm, which involves larger shared matrices and is inherently more complex. In this case, the Sherman-Morrison-Woodbury-based algorithmic optimization provides a maximum speedup of 4.45 \times , and the vector computing acceleration achieves 9.19 \times . Together, they yield a total speedup of 13.82 \times . Overall, increasing the size of context and action feature vectors enhances the advantage of vector parallel processing. The presented dual-pronged strategy effectively improves execution time and energy consumption, proving beneficial for deploying AI models in edge computing environments with low-power and real-time requirements.

6 Conclusions

In this work, we introduced a dual optimization strategy that combines algorithmic and hardware support techniques to cut down on the execution time and energy consumption of two LinearUCB Contextual Bandits algorithms, in the context of embedded learning systems. Using the Sherman-Morrison-Woodbury formula, we replaced intensive matrix inversions with efficient incremental updates, reducing memory requirements and computational complexity. Porting the code on the Klessydra-T13 RISC-V core's vector computing support, we expedited core matrix operations, improving speed and energy efficiency. To validate the proposed enhancements, we implemented and executed both traditional and optimized LinearUCB algorithms on the Cortex M4 STM32 platform, the Cortex A72 Raspberry Pi 4

Model B platform, and the RISC-V Klessydra-T13 PULPino platform, varying context and action feature vector sizes to evaluate execution speedup and energy reduction. The obtained results demonstrate substantial improvements, making this integrated approach highly suitable for embedded applications with stringent execution time and power consumption requirements, like learning systems on the edge of the Internet-of-Things.

References

- [1] Taiwo Samuel Ajani, Agbotiname Lucky Imoize, and Aderemi A Atayero. 2021. An overview of machine learning within embedded and mobile devices—optimizations and applications. *Sensors* 21, 13 (2021), 4412.
- [2] Fernando Amat, Ashok Chandrashekar, Tony Jebara, and Justin Basilico. 2018. Artwork Personalization at Netflix. In *Proceedings of the 12th ACM Conference on Recommender Systems* (Vancouver, British Columbia, Canada) (*RecSys '18*). Association for Computing Machinery, New York, NY, USA, 487–488. <https://doi.org/10.1145/3240323.3241729>
- [3] Marco Angioli, Marcello Barbirotta, Abdallah Cheikh, Antonio Mastrandrea, Francesco Menichelli, Saeid Jamili, and Mauro Olivieri. 2024. Design, Implementation and Evaluation of a New Variable Latency Integer Division Scheme. *IEEE Trans. Comput.* 73, 7 (2024), 1767–1779. <https://doi.org/10.1109/TC.2024.3386060>
- [4] Marco Angioli, Marcello Barbirotta, Abdallah Cheikh, Antonio Mastrandrea, and Mauro Olivieri. 2024. Exploring Variable Latency Dividers in Vector Hardware Accelerators. In *2024 19th Conference on Ph.D Research in Microelectronics and Electronics (PRIME)*, Vol. 1. Institute of Electrical and Electronics Engineers (IEEE), Larnaca, Cyprus, 1–4. <https://doi.org/10.1109/PRIME61930.2024.10559734>
- [5] Marco Angioli, Marcello Barbirotta, Antonio Mastrandrea, Saeid Jamili, and Mauro Olivieri. 2023. Automatic Hardware Accelerators Reconfiguration through LinearUCB Algorithms on a RISC-V Processor. In *2023 18th Conference on Ph.D Research in Microelectronics and Electronics (PRIME)*, Vol. 1. IEEE, Valencia, Spain, 169–172. <https://doi.org/10.1109/PRIME58259.2023.10161944>
- [6] Shahin Atakishiyev, Mohammad Salameh, Hengshuai Yao, and Randy Goebel. 2024. Explainable Artificial Intelligence for Autonomous Driving: A Comprehensive Overview and Field Guide for Future Research Directions. *IEEE Access* 12 (2024), 101603–101625. <https://doi.org/10.1109/ACCESS.2024.3431437>
- [7] Peter Auer, Nicolo Cesa-Bianchi, and Paul Fischer. 2002. Finite-time analysis of the multiarmed bandit problem. *Machine learning* 47, 2 (2002), 235–256.
- [8] Marcello Barbirotta, Abdallah Cheikh, Antonio Mastrandrea, Francesco Menichelli, Marco Angioli, Saeid Jamili, and Mauro Olivieri. 2023. Fault-Tolerant Hardware Acceleration for High-Performance Edge-Computing Nodes. *Electronics* 12, 17 (2023), 3574.
- [9] Marcello Barbirotta, Francesco Menichelli, Abdallah Cheikh, Antonio Mastrandrea, Marco Angioli, and Mauro Olivieri. 2024. Dynamic Triple Modular Redundancy in Interleaved Hardware Threads: An Alternative Solution to Lockstep Multi-Cores for Fault-Tolerant Systems. *IEEE Access* 12 (2024), 95720–95735. <https://doi.org/10.1109/ACCESS.2024.3425579>
- [10] Hamsa Bastani and Mohsen Bayati. 2020. Online decision making with high-dimensional covariates. *Operations Research* 68, 1 (2020), 276–294.
- [11] Djallel Bouneffouf, Irina Rish, and Charu Aggarwal. 2020. Survey on Applications of Multi-Armed and Contextual Bandits. In *2020 IEEE Congress on Evolutionary Computation (CEC)*. Institute of Electrical and Electronics Engineers (IEEE), Glasgow, United Kingdom., 1–8. <https://doi.org/10.1109/CEC48606.2020.9185782>
- [12] Sérgio Branco, André G Ferreira, and Jorge Cabral. 2019. Machine learning in resource-scarce embedded systems, FPGAs, and end-devices: A survey. *Electronics* 8, 11 (2019), 1289.
- [13] Lorenzo Canese, Gian Carlo Cardarilli, Luca Di Nunzio, Rocco Fazzolari, Daniele Giardino, Marco Re, and Sergio Spanò. 2021. Multi-agent reinforcement learning: A review of challenges and applications. *Applied Sciences* 11, 11 (2021), 4948.
- [14] Guillaume Chacun, Mehdi Akeddar, Thomas Rieder, Bruno Da Rocha Carvalho, and Marina Zapater. 2024. DroneBandit: Multi-armed contextual bandits for collaborative edge-to-cloud inference in resource-constrained nanodrones. In *Proceedings of the Great Lakes Symposium on VLSI 2024* (Clearwater, FL, USA) (*GLSVLSI '24*). Association for Computing Machinery, New York, NY, USA, 98–104. <https://doi.org/10.1145/3649476.3658720>
- [15] Abdallah Cheikh, Stefano Sordillo, Antonio Mastrandrea, Francesco Menichelli, Giuseppe Scotti, and Mauro Olivieri. 2021. Klessydra-T: Designing Vector Coprocessors for Multithreaded Edge-Computing Cores. *IEEE Micro* 41, 2 (2021), 64–71.
- [16] Lixing Chen, Jie Xu, Shaolei Ren, and Pan Zhou. 2018. Spatio-Temporal Edge Service Placement: A Bandit Learning Approach. *IEEE Transactions on Wireless Communications* 17, 12 (2018), 8388–8401. <https://doi.org/10.1109/TWC.2018.2876823>
- [17] Radu Ciucanu, Marta Soare, and Sihem Amer-Yahia. 2022. Implementing Linear Bandits in Off-the-Shelf SQLite. In *EDBT 2022: International Conference on Extending Database Technology, Short paper*. OpenProceedings, Edinburgh (online), United Kingdom, 388–392. <https://hal.science/hal-03547303>
- [18] David Cortes. 2021. contextualbandits: Contextual Bandit Algorithms. <https://github.com/david-cortes/contextualbandits/tree/master> Accessed: 2024-07-12.
- [19] R. Duncan. 1990. A survey of parallel computer architectures. *Computer* 23, 2 (1990), 5–16. <https://doi.org/10.1109/2.44900>
- [20] Audrey Durand, Charis Achilleos, Demetris Iacovides, Katerina Strati, Georgios D. Mitsis, and Joelle Pineau. 2018. Contextual Bandits for Adapting Treatment in a Mouse Model of de Novo Carcinogenesis. In *Proceedings of the 3rd Machine Learning for Healthcare Conference (Proceedings of Machine Learning Research, Vol. 85)*, Finale Doshi-Velez, Jim Fackler, Ken Jung, David Kale, Rajesh Ranganath, Byron Wallace, and Jenna Wiens

- (Eds.), PMLR, Palo Alto, California, 67–82. <https://proceedings.mlr.press/v85/durand18a.html>
- [21] Shicheng Guo, Xueyu Wei, Yun Xu, Wei Xue, Xuanguo Wu, and Bo Wei. 2022. A Survey of Linear Value Function Approximation in Reinforcement Learning. In *Exploration of Novel Intelligent Optimization Algorithms*, Kangshun Li, Yong Liu, and Wenxiang Wang (Eds.). Springer Nature Singapore, Singapore, 266–280.
- [22] William W Hager. 1989. Updating the inverse of a matrix. *SIAM review* 31, 2 (1989), 221–239.
- [23] Xu HE, Bo An, Yanghua Li, Haikai Chen, Qingyu Guo, Xin Li, and Zhirong Wang. 2020. Contextual User Browsing Bandits for Large-Scale Online Mobile Recommendation. In *Proceedings of the 14th ACM Conference on Recommender Systems (Virtual Event, Brazil) (RecSys '20)*. Association for Computing Machinery, New York, NY, USA, 63–72. <https://doi.org/10.1145/3383313.3412234>
- [24] Matt Johns and Tom J. Kazmierski. 2020. A Minimal RISC-V Vector Processor for Embedded Systems. *2020 Forum for Specification and Design Languages (FDL)* 1 (2020), 1–4. <https://api.semanticscholar.org/CorpusID:226265202>
- [25] Wali Ullah Khan, Muhammad Awais Javed, Sherali Zeadally, Eva Lagunas, and Symeon Chatzinotas. 2023. Intelligent and Secure Radio Environments for 6G Vehicular Aided HetNets: Key Opportunities and Challenges. *IEEE Communications Standards Magazine* 7, 3 (2023), 32–39. <https://doi.org/10.1109/MCOMSTD.0007.2200065>
- [26] Lihong Li, Wei Chu, John Langford, and Robert E. Schapire. 2010. A contextual-bandit approach to personalized news article recommendation. In *Proceedings of the 19th International Conference on World Wide Web (Raleigh, North Carolina, USA) (WWW '10)*. Association for Computing Machinery, New York, NY, USA, 661–670. <https://doi.org/10.1145/1772690.1772758>
- [27] Michael L Littman. 2015. Reinforcement learning improves behaviour from evaluative feedback. *Nature* 521, 7553 (2015), 445–451.
- [28] Timothy A Mann, Hugo Penedones, Shie Mannor, and Todd Hester. 2016. Adaptive lambda least-squares temporal difference learning. arXiv:1612.09465 [cs.LG] arXiv preprint arXiv:1612.09465.
- [29] MG Sarwar Murshed, Christopher Murphy, Daqing Hou, Nazar Khan, Ganesh Ananthanarayanan, and Faraz Hussain. 2021. Machine learning at the network edge: A survey. *ACM Computing Surveys (CSUR)* 54, 8 (2021), 1–37.
- [30] Elias D Nino Ruiz, Adrian Sandu, and Jeffrey Anderson. 2015. An efficient implementation of the ensemble Kalman filter based on an iterative Sherman–Morrison formula. *Statistics and Computing* 25 (2015), 561–577.
- [31] Ricardo Silva Peres, Xiaodong Jia, Jay Lee, Keyi Sun, Armando Walter Colombo, and Jose Barata. 2020. Industrial artificial intelligence in industry 4.0-systematic review, challenges and outlook. *IEEE Access* 8 (2020), 220121–220139.
- [32] Guoguang Rong, Arnaldo Mendez, Elie Bou Assi, Bo Zhao, and Mohamad Sawan. 2020. Artificial intelligence in healthcare: review and prediction case studies. *Engineering* 6, 3 (2020), 291–301.
- [33] Jack Sherman and Winifred J Morrison. 1950. Adjustment of an inverse matrix corresponding to a change in one element of a given matrix. *The Annals of Mathematical Statistics* 21, 1 (1950), 124–127.
- [34] Ambuj Tewari and Susan A. Murphy. 2017. *From Ads to Interventions: Contextual Bandits in Mobile Health*. Springer International Publishing, Cham, 495–517. https://doi.org/10.1007/978-3-319-51394-2_25
- [35] Chien-Sheng Yang, Ramtin Pedarsani, and A Salman Avestimehr. 2021. Edge computing in the dark: Leveraging contextual-combinatorial bandit and coded computing. *IEEE/ACM Transactions on Networking* 29, 3 (2021), 1022–1031.
- [36] ZOZO Research. 2021. zr-obp: Open Bandit Pipeline. <https://github.com/st-tech/zr-obp/tree/master> Accessed: 2024-07-12.